

## Induction surface hardening – comparison of different methods

**Abstract.** The overview of the induction surface hardening methods were presented in the paper. Two examples are considered: continual hardening of cylinders made of steel 38Mn6 and dual frequency hardening of gear wheels made of steel 40 HNMA. Results of measurements provided at the experimental stand were presented. Acceptable accordance between measurements and numerical computations were obtained. Final conclusions were formulated. (Hartowanie indukcyjne powierzchniowe – porównanie różnych metod)

**Streszczenie.** W pracy dokonano przeglądu metod hartowania indukcyjnego powierzchniowego elementów stalowych. Rozpatrzono dwa przypadki: hartowania przelotowego wałków ze stali 38Mn6 oraz hartowania dwuczęstotliwościowego kół zębatach ze stali 40HNMA. Przedstawiono wyniki pomiarów na stanowisku doświadczalnym. Uzyskano zadowalającą zbieżność między wynikami pomiarów i obliczeń numerycznych. **Przegląd metod hartowania indukcyjnego powierzchniowego elementów stalowych**

**Keywords:** induction surface hardening, induction heating, continual hardening, dual frequency hardening.

**Słowa kluczowe:** hartowanie indukcyjne powierzchniowe, nagrzewanie indukcyjne, hartowanie ciągłe, hartowanie dwuczęstotliwościowe

### Introduction

Induction surface hardening (ISH) is a kind of the induction hardening which causes changes in the crystalline microstructure resulting in their higher hardness of surface zones of steel bodies only. Their internal parts remain unchanged and soft. In general, in order to obtain such a microstructural transformation the body is heated first inductively in the high frequency electromagnetic field. Surface zones of the body reach the assumed hardening temperature  $T_h$  which secures a completion of the austenitic microstructure, while in internal zones temperature is too low for such the transformation. Immediately after heating, or after very short austenitization break (being of the milliseconds order), the body is intensively cooled in a selected quenchant (water, spray being a suitable mixture of water and air, oil or polymer liquids). Such a technology makes possible to generate extremely high power density in the thin hardened zone due to application of modern high frequency transistor sources and because of short heating times [1]. The ISH is modern, energy-efficient and environment-friendly heat treatment technology very effective in comparison with classical surface hardening methods as for instance carbonizing. It is especially often applied for axi-symmetric or flat workpieces, however recently it used also for elements of complex shapes [2]. The advantage of the ISH technology is connected with a location the energy source very close to the hardened zone. Its thickness could be regulated. For instance in order to obtain very thin hardened depth high frequency single frequency induction hardening system is applied. In order to achieve contour profile for hardening of gear wheels dual frequency induction hardening system could be used [3].

Based upon a short description of the ISH two particular examples are presented and discussed in the paper: continual hardening of cylinders made of steel 38Mn6 and dual frequency hardening of gear wheels made of steel 40 HNMA. Mathematical modeling of the ISH process is described for instance in [4]. Computations of hardness distribution were compared with measurements and satisfactory accuracy was achieved.

### Idea of ISH process

Let us consider shortly the idea of the ISH process. It consists of three consecutive stages: rapid induction heating, extremely short austenitization and cooling. Heating could be realized in one or in two cycles. Exemplary temperature dependence on time for single frequency process (SFIH) is presented in Fig. 1. The time

of induction heating  $t_{ih}$  is short (a couple of seconds or even hundreds of milliseconds). The average temperature exceeds the modified upper critical temperature  $Ac_{3m}$  and reach final value of about the hardening temperature  $T_h$ .

$$(1) \quad Ac_{3m} \leq T|_{t=t_{ih}} \leq T_h$$

The austenitization time  $t_a$  means a time necessary for switching off the inductor and start cooling. However even for such a short time temperature distribution could decrease. In order to secure completion of austenite microstructure the inequality (2) should satisfy

$$(2) \quad T|_{t=t_{ih}+t_a} \geq Ac_{3m}$$

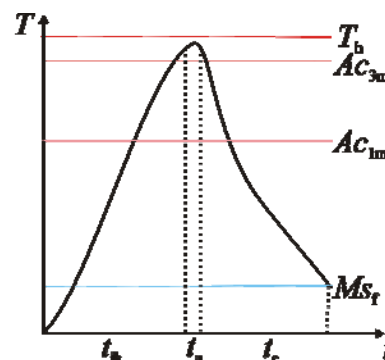


Fig.1. Exemplary temperature dependence on time in surface zone of the body for the SFIH process (Notations in text)

Deeper parts of the body are heated to temperature which exceed the lower critical temperature  $Ac_{1m}$ , but do not reach the upper critical temperature  $Ac_{3m}$

$$(3) \quad Ac_{3m} \geq T|_{t=t_{ih}+t_a} \geq Ac_{1m}$$

The austenite transformation begins, but it is not completed. For internal parts of the body the temperature does not reach even the modified lower critical temperature  $Ac_{1m}$

$$(4) \quad T|_{t=t_{ih}+t_a} \leq Ac_{1m}$$

and the austenite transformation does not begin at all. As a final result after intensive cooling with the velocity  $v_c$  bigger than its critical value  $v_{cmin}$  to the temperature smaller than the martensite finish temperature  $Ms_f$

$$(5) \quad v_c > v_{cmin} \quad T|_{t=t_{ih}+t_a+t_c} < Ms_f$$

we obtain thin surface zone with fully hardened material having martensitic microstructure, then partly hardened transition zone with a mixed microstructure containing not only martensite and not solved ferrites, pearlites and carbides and not hardened internal zone with prior, unchanged microstructure.

Exemplary temperature dependence on time for consecutive dual frequency process (CDFIH) is presented in Fig. 2.

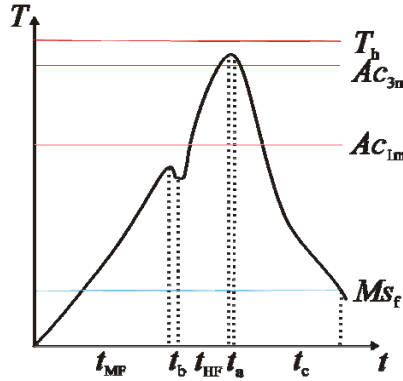


Fig.2. Exemplary temperature dependence on time in surface zone of the body for the CDFIH process (Notations in text)

The CDFIH process means first medium frequency induction heating (time  $t_{MF}$ ) to the temperature lower than the modified lower critical temperature

$$(6) \quad T|_{t=t_{MF}} < Ac_{1m}$$

The next step is the high frequency induction heating (time  $t_{HF}$ ). The break (time  $t_b$ ) between two steps of heating is as small as possible. The final temperature satisfies inequality (7).

$$(7) \quad T|_{t=t_{MF}+t_b+t_{HF}+t_a} \geq Ac_{3m}$$

The CDFIH is terminated with the intensive cooling.

### Parameters influencing on hardness distribution

The main parameters characterized quality of the ISF process are microstructure and thickness of the hardened zone. The thickness  $\Delta_g$  is defined as the distance from the surface with 80 % of the requested surface hardness. Its microstructure at the border may contain of about 50% of martensite. Typically the hardness decreases to the value of about in Rockwell degrees 45 – 50 (HRC). It depends on many factors. Correct selection of four of them seems to be more important:

- frequency of inductor current,
- surface power density delivered to the body,
- heating time and correct critical temperatures,
- intensity of cooling.

Designing of heating and cooling systems are the task-specific one. Testing of its design and construction is crucial. It takes repeated testing to achieve optimal shape of temperature distribution and consequently the expected hardness depth.

Depth of hardening is mostly the assumed value being the basis for a computation of all parameters of the heating and cooling systems.

Frequency of inductor current could be selected in broad ranges given by inequality (8) [5].

$$(8) \quad \frac{0.015}{\Delta_g^2} < f < \frac{0.25}{\Delta_g^2}$$

Selection of such defined frequency is based upon assumed value of the hardening depth. For instance for  $\Delta_g = 10^{-3}$  m: (16 kHz <  $f$  < 250 kHz). Dependence of the critical temperatures on heating rate are determined from the Time-Temperature-Austenitization (TTA) diagram for investigated steel. Exemplary dependence of critical temperatures on heating rate for the quenched-and-tempered steel (Q&T) 40 HNMA is presented in Fig. 3.

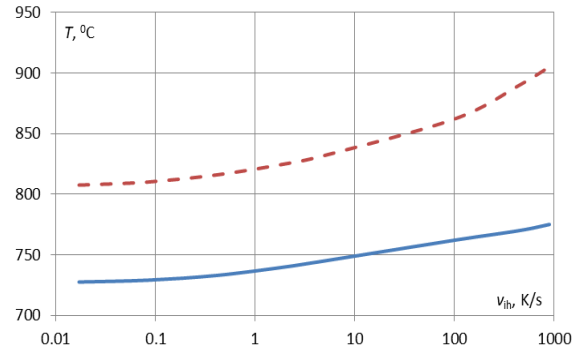


Fig.3. Exemplary dependence of the critical temperatures  $Ac_{1m}$  and  $Ac_{3m}$  on heating rate for the steel NiCrMo (40 HNMA)

For the low heating rate  $v_{in} = 0.016$  K/s the modified upper critical temperature  $Ac_{3m1} = 807.5^{\circ}C$  and it is almost the same value as for the conventional slow heating in furnaces. If the heating rate is distinctly bigger ( $v_{in} = 900$  K/s) the modified upper critical temperature  $Ac_{3m2} = 901^{\circ}C$  and it is 93.5 K higher than  $Ac_3$ . In the same conditions as previously the modified lower critical temperature  $Ac_{1m1} = 727.5^{\circ}C$  and  $Ac_{1m2} = 790^{\circ}C$  and it is 62.5 K of difference between them. For the hardening process important influence have also four other parameters which should recognized well for planned induction hardening process. The first of them is the prior microstructure [6]. The second strongly influencing parameter is the magnetic permeability of steel which changes rapidly because of magnetic transformation at the temperature of Curie point  $Ac_2$  [7]. The third one is inaccuracy of temperature characteristics of material properties and heat transfer coefficients [8]. An incorrect value of such properties like electric conductivity, density, thermal conductivity and specific heat could cause differences of calculated final temperature of about 100 K [9]. And finally a way of cooling and the cooling rate. Exemplary dependence of hardness on the cooling rate determined from the Cooling-Time-Temperature continuous (CTTc) diagram for steel 40 HNMA is presented in Fig.4. The uniform martensitic microstructure at the surface zone is obtained if the cooling rate is big enough and the final temperature  $T_f$  in the whole hardened zone is smaller than the martensite finish temperature  $Ms_f$ .

### Overview of the ISH methods

The paper presents the overview analysis of different ISH methods and gives some examples of their practical application. In general ISH methods could be divided into two groups:

- Continual induction surface hardening CISH,
- Spin induction surface hardening SISH.

Long elements require continual way of induction hardening. Then there are workpieces whose irregular shapes or complex geometries makes spin hardening as

the only possible arrangement. Below a short description of both methods is presented.

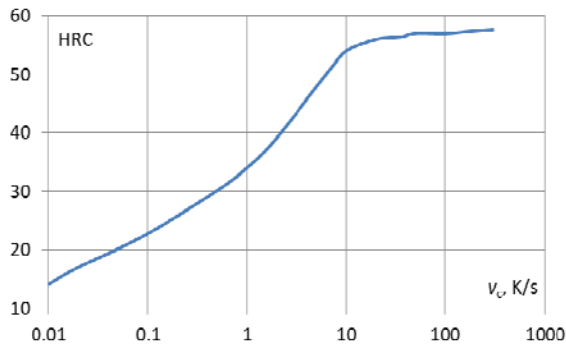


Fig. 4. Exemplary dependence of hardness on cooling rate for steel 40 HNMA

The CISH means relative movement between the body and the inductor-sprayer system. It is divided into vertical, horizontal or circumferential kind of the heat treatment. For the vertical process the body is held stationary in a vertical position and the inductor (or body) moves with velocity in the range of about 0.001 - 0.05 m/s. An advantage of the CISH process is a quite simple construction of the inductor. Typically it is one turn coil often equipped with a flux concentrator. Another advantage is a fact that the sprayer is placed exactly below the inductor. The quenchant flows directly downward without any contact with the heating area. It is possible to control the depth of hardening in different zones of the body. An advantage of horizontal hardening is connected with facilitation of treatment of large bodies. It makes possible, for example, to harden conical mandrels [10] or tubes up to 2 m or more long with this method [11]. A variant of both previous methods is the circumferential SCIH process. A good example of such the process is Part-by Part Induction Hardening (PIIH) of circular saw applied for cutting of slabs in continuous casting lines of steel [12]. In the first step the inductor covers a small part of the saw only (for instance 3-4 teeth). In the next step the inductor was removed to the next position and teeth heated in the previous step are now cooled. The shifting of the induction-sprayer system is continued until the hardening process was completed. In case of gear wheels with modulus  $m > 6$  the Tooth by Tooth Induction Hardening (TTIH) was often applied. Two different types of inductors could be used. In the first step the inductor heats up the first tooth. In the next step the inductor was removed to the next tooth and the tooth heated in the previous step is cooled. The shifting of the induction-sprayer system is continued until the hardening process was completed.

The SISH means the complete hardening zone is first heated and then quenched. Such a hardening can be achieved with a single or multi-turn coil that encircles the entire hardened zone. The benefit the SISH include minimized distortion and optimal results for workpieces with complex geometries and/or large diameter changes. The method's relatively long heating times and distinctly bigger power (compared to scanning) also benefit the workpiece microstructure and residual stresses. But even if single-shot's heating time for each grain is longer compared to scanning, the total heating time is shorter since the entire heating zone is heated at the same time. Single-shot hardening typically requires more power than scanning. This extra power is needed to achieve the required temperature increase in the complete hardening zone. Moreover, the coils used in spin hardening are more complicated and expensive than those used previously.

And if the power demand changes somewhere on the workpiece, it will be necessary to physically modify the inductor. There are different induction surface hardening methods for gear wheels. Accordingly to requested hardening patterns. It is realized in a different arrangements and supply systems

- single frequency induction hardening SFIH,
- consecutive dual frequency induction hardening CDFIH,
- simultaneous dual frequency induction hardening SDFIH.

Accordingly to requested hardening patterns different methods are used (Fig. 5). The hardness pattern (fully hardened tooth) shown in Fig. 5a is characteristic for medium frequency (MF) SFIH process. If the inductor is supplied from the high frequency generator (HF) the hardness pattern is completely different Fig. 5b). Only the root of the tooth is hardened with the root kept soft. The CDFIH process makes possible to obtain the contour hardness pattern (Fig. 5c) with the almost uniform thin hardened zone. The gear wheel is heated first by the MF inductor to the modified lower critical temperature  $Ac_{1m}$ , then by the HF inductor to the hardening temperature  $T_h$  and finally immediately cooled. The similar hardness profile could be obtained if the heating is simultaneous [13].

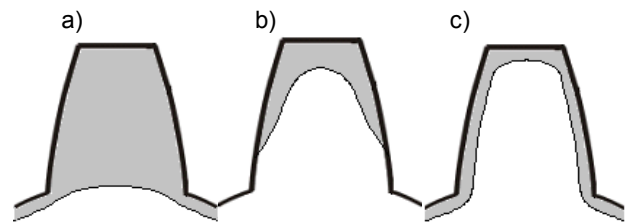


Fig. 5. Profile of hardened zone a) through tooth hardening, b) local root hardening, c) contour hardening

### Examples of application

Let us consider first as an example of the SSIH process provided for the steel element used in machinery industry. The toothed cylindrical element is shown in Fig. 6a. It is made of steel 38Mn6. Its chemical composition was collected in Tab. 1.

Table1. Chemical composition of steel 38 Mn6

Element	C	Mn	Si	Cr	Mo	Ni
% mass.	0.37-0.42	1.2-1.6	max 0.25	max 0.25	Max 0.1	Max 0.15

The dimensions of the treated element are as follow: length with toothed part  $l = 85$  mm, length of cylindrical part  $l_c = 52$  mm, length of expected hardened zone  $l_h = 40$  mm, diameter of toothed and cylindrical part respectively  $D_t = 12$  mm,  $D_c = 8$  mm. Expected thickness of the hardened layer is equal to 0.6 mm with hardness of about 51 – 59 HRC. The arrangement of the SSIH system is presented in Fig. 5b. The vertically located element 2 is heated by the moving cylindrical inductor 1. Velocity of movement is regulated in order to achieve requested temperature distribution within the hardened layer satisfying condition (1). Then heated part of the element 2 is cooled by the sprayer 3. As a quenchant 4 the polymer solution Aqua Quench 140 is applied. In order to minimize electrical losses distance between bus-bars 5 is as minimal as possible. Basic dimensions of inductor-sprayer system: height of one-turn inductor  $h = 10$  mm, its width  $b = 5$  mm, internal diameter  $D_i = 18$  mm, external diameter  $D_e = 30$  mm, internal diameter of sprayer 37 mm.

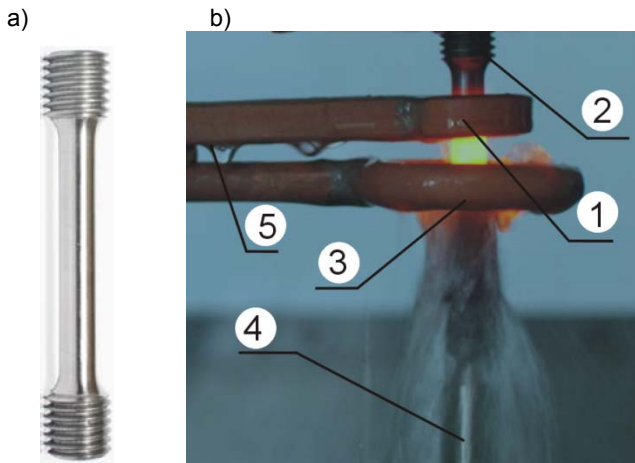


Fig. 6. Element (a) and arrangement of the inductor-sprayer-element system (b). 1 – inductor, 2 – element, 3 – sprayer, 4 – quenchant, 5 – bus-bars.

The material is in the heat refined state. And its prior microstructure is characterized by mixture of pearlite and ferrite particles (Fig. 7).

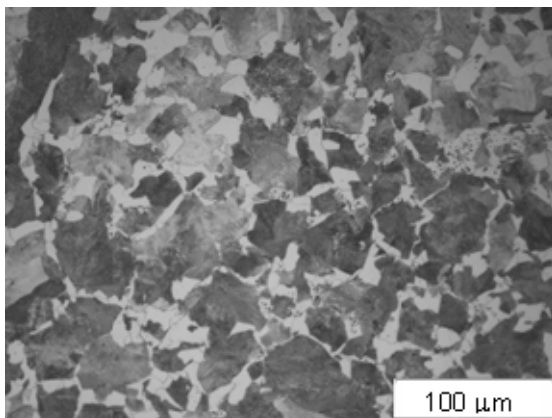


Fig. 7. Prior microstructure of steel 38Mn6 in condition after heat refining (mag x500)

Several simulations are provided by means of 2D Flux software [14]. Computations are verified by measurements realized at the specialized laboratory stand located in the Silesian University of Technology. Quite reasonable accordance between calculated and measured temperature in selected points of the cylinder surface was obtained [15]. Measured hardness distribution in radial direction at the middle cross-section of the element and microstructure of the hardened layer are shown in Fig. 8 and Fig. 9 respectively [16]. The thickness of the hardened layer  $\Delta_u$  with martensitic microstructure (Fig. 8) and hardness of 51 HRC and more is equal to 0.6 mm.

The transition, partly hardened layer with hardness between 30 – 51 HRC and with mixed martensite and bainite microstructure has thickness of about 0.7 mm (distance to the surface changes between 0.6 mm and 1.3 mm). If the distance is bigger than 1.3 mm we have internal zone with unchanged pearlite-ferrite microstructure and hardness smaller than 30 HRC. But defined hardening depth  $\Delta_g = 1$  mm.

Let us consider an example of the CDFIH process provided for the small gear wheel with following dimensions: teeth number  $n = 16$ , width of the tooth ring  $b = 6$  mm, root diameter  $d_e = 35.6$  mm, tip diameter  $d_t = 26.9$  mm, hole diameter  $d_h = 0.016$  m. It is made of non-alloy

steel for quenching and tempering 40 HNMA. Its chemical composition is presented in Table 2

Table 2. Chemical composition of steel 40 HNMA

Element	C	Mn	Si	Ni	Cr
% mass	0.37 – 0.44	0.5 – 0.8	0.17 – 0.37	1.25 – 1.6	0.6 – 0.9

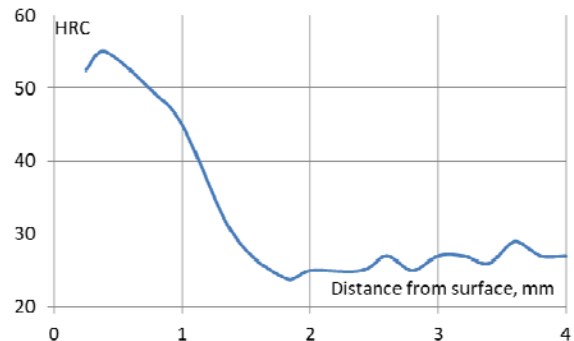


Fig. 8. Dependence of hardness on distance from the surface

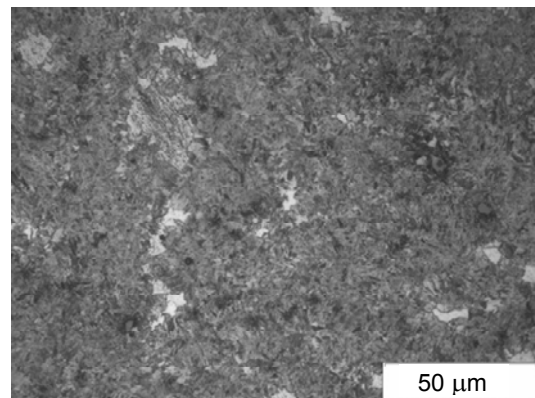


Fig. 9. Microstructure in the distance of 0.2 mm from the surface depicted in the top of the tooth. Martensite (grey) with single retained austenite (white) (mag x1000)

The arrangement of the CDFIH system is presented in Fig.10. At beginning the gear wheel 3 is located inside the MF inductor 1 and heated to the temperature of about the lower critical temperature  $Ac_{1m}$ . Then it is quickly removed to the next position inside the HF inductor equipped with the flux concentrator. When the temperature exceeds the assumed hardening temperature  $T_h$  gear is removed to the final position inside sprayer 4. As a quenchant the same polymer solution Aqua Quench 140 as previously is applied. In order to obtain expected hardness distribution along external diameter of the element the gear wheel mounted on cylinder 5 rotates with velocity of about 3 – 5 r/s. In order to minimize electrical losses lengths and distances between MF bus-bars 6 and HF bus-bars 7 are as minimal as possible. Basic dimensions of the inductor-sprayer system are as follow: MF inductor: number of turns  $n = 1$ , height  $h_{MF} = 10$  mm, internal diameter  $d_i = 39.5$  mm, external diameter  $d_e = 54$  mm, HF inductor: number of coils  $N = 1$ , height of coil  $H_{HF} = 7$  mm, total height including magnetic flux concentrator  $H_t = 21$  mm, external diameter  $D_e = 61$  mm, internal diameter  $D_i = 39.5$  mm, sprayer: internal diameter  $d_s = 64$  mm. Computations are provided by means of 3D Flux software for coupled electromagnetic and temperature field during induction heating and cooling and QT steel software supported by several own procedures for hardness and microstructure fields.

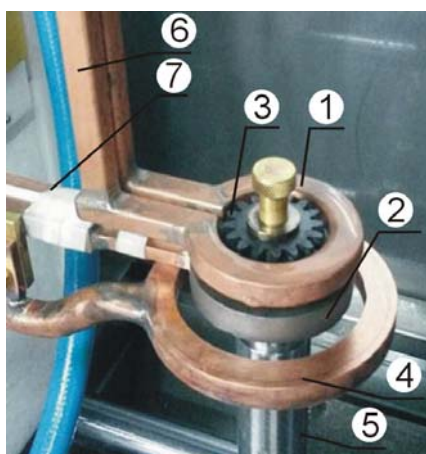


Fig. 10. Arrangement of CDFIH system 1 – MF inductor, 2 – HF inductor with flux concentrator, 3 – gear wheel, 4 – sprayer, 5 – cylinder, 6 – MF bus-bars, 7 – HF bus-bars

Prior microstructure of the material is presented in Fig. 11. Several computations are provided also for different kind of NiCrMo steel.

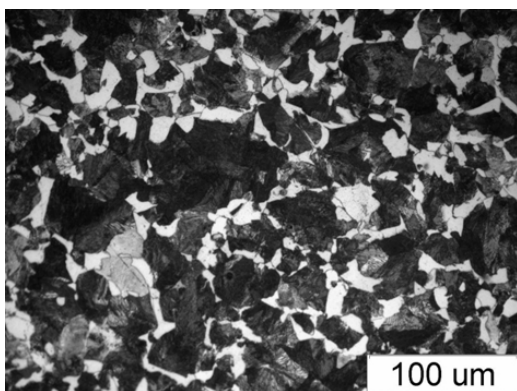


Fig. 11. Prior microstructure of steel 40HNMA in condition of normalizing (mag x 500)

There are presented and discussed in details for instance in [17 - 21]. Multi variant computations make possible to recognize correct parameters and shorten a time necessary to find optimal parameters during experiments provided on the specialized laboratory stand located in the Silesian University of Technology in Katowice. In order to avoid internal stresses after induction hardening each gear wheel is tempered in a resistance chamber furnace in temperature of about 160°C during 1 – 2 hours. Let choose points A - G located at the working surface of the tooth (Fig.12). Hardness distribution along the line AG is presented in Fig. 13.

Hardness along the line AG is not fully uniform, but difference between points A and G is equal to 8.5 HRC and it matches requirements. However checking of hardness distribution of the working surface of the tooth is not enough. Expected fully hardened zone with a martensite microstructure should have a contour shape similar to this shown in Fig. 5c. Hardness in Rockwell degrees was measured by the micro-hardness tester FM 700.

In order to check it the hardness was measured along three lines shown in Fig. 14. Measured hardness distribution in direction of depth of the material along lines 1 and 2 crossing the tooth space perpendicular in point A and top of the tooth in point G respectively are presented in Fig. 15.

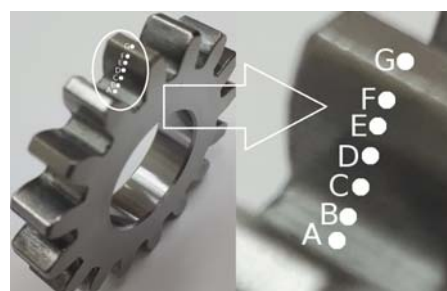


Fig. 12. Investigated gear wheel, A...G points at the working surface of the gear wheel

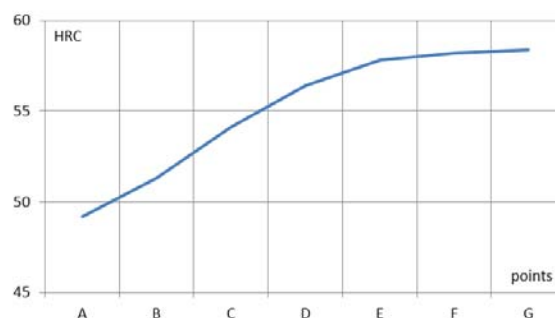


Fig. 13. Hardness distribution along at the working surface at points A...G in Rockwell degrees HRC

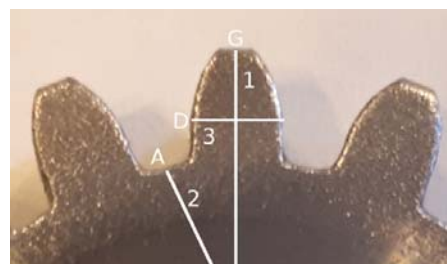


Fig. 14. Location of lines 1, 2, 3 on tooth of the gear wheel

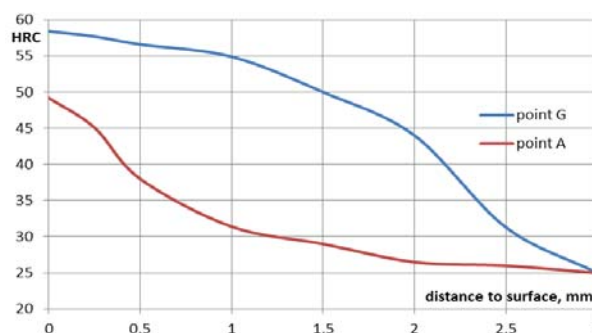


Fig. 15. Hardness distribution at the space area along line 1 crossing point A and line 2 crossing point G (their location are shown in Fig. 12)

Based upon presented curves 1, 2 the hardness depth for space and top of the tooth respectively are determined. For the space of the tooth (point A) the thickness of hardened zone is equal to 0.25 mm. For the top of the tooth (point G) the thickness of hardened zone is equal to 1.85 mm. So the shape of the contour hardened zone matches the requirements however expected thickness of the contour zone along the working surface should be equal to 1 mm, but it is non-uniform. In order to learn more about the shape of the curve hardness is measured also in along line 3 crossing the point D along a line parallel to the top plane of the tooth (Fig. 16).

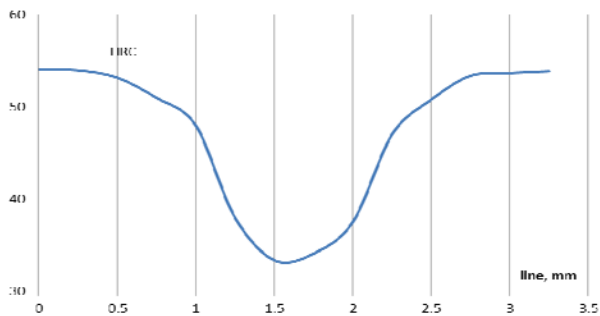


Fig. 16. Hardness distribution at the working surface of the tooth along line 3 crossing point D (see Fig.14)

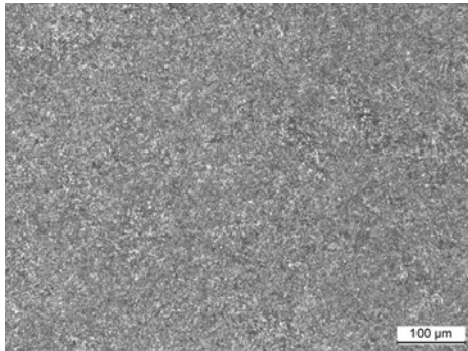


Fig. 17. Microstructure in the distance of 0.2 mm from the surface depicted in the top of the tooth. Martensite with single retained austenite (mag x1000)

Measurements are compared with computations and quite reasonable accordance between them was achieved.

### Conclusion

Induction hardening belongs to modern technology making possible to apply energy efficient and environment-friendly heat treatment method to a wide sort of steel elements well known for many years. The main factors deciding about efficiency of the induction hardening methods seems to be the elaboration of good, but simple computation methods supported by well-planned experiments making possible to design induction hardening systems. For calculation of such systems the available professional software supplemented by several singled owned procedures could be applied. However the important factors deciding about effectiveness of the applied methodology are also:

- well prepared input data like material properties and their temperature dependencies for the investigated steel,
- measured corrected values of the modified critical temperatures for real induction hardening conditions.

Material properties should be first determined based upon available databases or better directly by measurements. In case of the modified critical temperatures their values could be determine by measurements done at samples of the material for real heat treatment conditions.

### Acknowledgment

The paper was prepared within the NCBiR project PBS2/A5/41/2014

**Author:** prof. dr hab. inż. Jerzy Barglik, Politechnika Śląska, Katedra Informatyki Przemysłowej, ul. Krasińskiego 8, 40-019 Katowice E-mail: [jerzy.barglik@polsl.pl](mailto:jerzy.barglik@polsl.pl).

### REFERENCES

- [1] Rudnev V., Loveless D., Cook R., L., Handbook of Induction Heating. *Second Edition, CRC Press. Taylor and Francis Group*, (2017), p. 730
- [2] Rudnev, V., Totten, G. Induction Heating and Heat Treatment, *ASM International*, 4C (2014), p. 820
- [3] Barglik J., Induction heating of technological processes. Heat Treatment. Mathematical modelling and Experimental Verification. Nagrzewanie indukcyjne w procesach technologicznych. Obróbka cieplna. Modelowanie matematyczne i weryfikacja doświadczalna. *Printed House of the Silesian University of Technology in Gliwice* (in Polish) (2015), p. 177
- [4] Barglik J., Mathematical modelling of induction surface hardening, *COMPEL* 35 (2016), n. 4, 1403 – 1417
- [5] Sajdak C., Samek E., Induction Heating *Śląsk*, (1987) p.360 (in Polish)
- [6] Rudnev V., The day after tomorrow – the future of induction heating, *Heat Processing* (2017) n. 4, 45 – 52
- [7] Barglik J., Smalcerz A., Influence of the magnetic permeability on modelling of induction surface hardening. *COMPEL-The international journal for computation and mathematics in electrical and electronic engineering* 36 Issue 2, (2017), 555 – 564
- [8] Schubotz S., Nacke B., Modeling and verification of convective heat transfer coefficient for induction applications, *International Journal for Electromagnetics and Mechanics*, 53, (2017), 79 – 88
- [9] Barglik J., Smagór A., Smalcerz A., Computer simulation of single frequency induction surface hardening of gear wheels: analysis of selected problems *International Journal of Microstructure and Material Properties* (2018) (in print)
- [10] Barglik J., Doležel I., Karban P., Continual induction hardening of 3D steel bodies of specific geometries *Przegląd Elektrotechniczny* (2007) nr 3, 75-77
- [11] Barglik J., Induction Hardening of Steel Tubes by Means of Internal Inductor, *Journal of Iron and Steel Research International*, 19, (2012) Supplement 1-2, 722 – 725
- [12] Barglik J., Dolezel I., Ducki K., Ulrych B., Mathematical and computer modelling of induction heating and consequent hardening of circular saw, *Chapter in book Electromagnetic Fields in Electrical Engineering, Studies in Applied Electromagnetics and Mechanics*. 22 (2002), 351 - 356
- [13] Lupi S., Fundamentals of Electroheat, *Electrical Technologies for Process Heating. Springer. Switzerland* (2017)
- [14] User Guide Flux 12 General tools, Geometry & mesh, Vol. 1, CEDRAT, (2015)
- [15] Barglik J., Smalcerz A., Smagór A., Paszek P., Analysis of continuous induction hardening of steel cylinder element made of steel 38Mn6, *Archives of Metallurgy and Materials*, 60 (2015), n. 4, 2855 – 2860
- [16] Smalcerz A., Barglik J., Kuc D., Ducki K., Wasiński S., The microstructure and mechanical properties of cylindrical elements from steel 38Mn6 after continuous induction heating, *Archives of Metallurgy and Materials*, 61 (2016), n. 4, 1969-1974
- [17] Lupi S., Forzan M., Alifirov A., Induction and direct resistance heating. Theory and numerical modelling, *Springer*, (2015),
- [18] Spezzapria M., Forzan M., Dughiero F., Numerical Simulation of Solid-Solid Phase Transformations During Induction Hardening, *IEEE Transactions of Magnetics*, 52 (2016), n. 3, 740 – 743
- [19] Schlesselmann D., Nikanorov A., Nacke B., Galunin S., Schon M., Yu Z., Numerical calculation and comparison of temperature profiles and martensite microstructures in induction surface hardening process, *International Journal for Electromagnetics and Mechanics*, 44 (2014), 137 – 145
- [20] Barglik J., Przyłucki R., Smalcerz A., Doležel I., 3D Modeling of Induction Hardening of Gear Wheels. *J. of Computational and Applied Mathematics*, 270 (2014) 231 – 240
- [21] Barglik J., Induction hardening of steel elements with complex shapes, *Przegląd Elektrotechniczny* 94 (2018) n.4, 51 – 54